

Energy Levels in Ne^{20} from the $\text{F}^{19}(d,n\gamma)\text{Ne}^{20}$ Reaction

J. W. BUTLER

Nucleonics Division, U. S. Naval Research Laboratory, Washington, D. C.

(Received October 21, 1959)

The gamma-ray threshold technique has been used with the $\text{F}^{19}(d,n\gamma)\text{Ne}^{20}$ reaction to find excited states in the residual nucleus, Ne^{20} . Thin targets of CaF_2 were bombarded with deuterons from a 2-Mv Van de Graaff accelerator. Two NaI(Tl) crystals (1.75-in. \times 1.75-in. and 3-in. \times 3-in.) were used in a coincidence arrangement to measure the gamma rays as a function of deuteron energy. Nine gamma-ray or neutron thresholds were found, at bombarding energies of 0.51 ± 0.02 , 0.60 ± 0.02 ?, 0.76 ± 0.02 , 0.85 ± 0.02 ?, 1.15 ± 0.02 , 1.35 ± 0.02 , 1.70 ± 0.02 , 1.79 ± 0.02 , and 2.06 ± 0.02 Mev. These threshold energies correspond to excited states in Ne^{20} at 11.11 ± 0.02 , 11.19 ± 0.02 ?, 11.33 ± 0.02 , 11.42 ± 0.02 ?, 11.69 ± 0.02 , 11.87 ± 0.02 , 12.19 ± 0.02 , 12.27 ± 0.02 , and 12.51 ± 0.02 Mev, respectively. All of these states decay principally to the ground state of Ne^{20} except the 11.11-, 11.19-, and 12.27-Mev states, which decay primarily to the 1.63-Mev state. Possible isobaric spin assignments are discussed.

I. INTRODUCTION

THE success of the shell model in predicting the spacing and other properties of excited states for nuclides in the vicinity of doubly closed shells makes it highly desirable to obtain more data on such nuclides. For some years a great deal has been known about the level structure of Ne^{20} , except for the region from 10 to 13 Mev.

The region of excitation in Ne^{20} below 10 Mev is accessible by means of a number of nuclear reactions: $\text{O}^{16}(\alpha,\alpha)$, $\text{O}^{16}(\alpha,\gamma)$, $\text{Ne}^{20}(x,x')$, $\text{Na}^{23}(p,\alpha)$, and $\text{F}^{19}(d,n)$. The region above 13 Mev is accessible by means of the proton bombardment of F^{19} . The region between about 10 and 13 Mev is not easily accessible by any of these reactions. States in this region can be excited by means of the $\text{F}^{19}(d,n)$ reaction, but conventional methods in neutron spectroscopy are inadequate to resolve the neutron groups leading to states in Ne^{20} from 10 to 13 Mev. The high bombarding energy required for the $\text{Na}^{23}(p,\alpha)$ reaction to excited states in this region makes resolution of the different alpha-particle groups leading to these states likewise impractical, at least up to the present time.

The use of neutron threshold techniques with the $\text{F}^{19}(d,n)\text{Ne}^{20}$ reaction offers a means of detecting excited states in this region of excitation in Ne^{20} , but because of the large number of neutron groups having positive Q values, the detection sensitivity of conventional neutron threshold techniques is not sufficient for definite identification of any slow neutron thresholds in this reaction.^{1,2}

In order to measure the energies of excited states in this region of Ne^{20} (10–13 Mev), a “gamma-ray threshold” detection technique was developed and used with the $\text{F}^{19}(d,n\gamma)\text{Ne}^{20}$ reaction. This technique has since been used to find neutron thresholds in the $\text{O}^{18}(d,n\gamma)\text{F}^{19}$ reaction. These later experiments have been reported.^{3,4}

and the “gamma-ray threshold” technique described in detail.

The essential element of the gamma-ray threshold detection technique is the use of a gamma-ray spectrometer (for example, a NaI crystal with associated differential pulse-height analyzer). The spectrum of gamma rays is taken at each bombarding energy chosen. The appearance of a new gamma ray (as a function of bombarding energy) marks the threshold for a new neutron group leading to the state which decays by emitting this new gamma ray (perhaps along with others).

If the over-all yield of gamma rays is increasing rapidly with bombarding energy (because of the energy dependence of Coulomb barrier penetrabilities), it is sometimes desirable to eliminate this energy dependence of the yield by dividing the counts in each channel of a differential pulse height analyzer by the total number of counts in all channels. This “normalization” process therefore makes the average yield constant as a function of energy. Thus if a new gamma ray appears, it can be seen as a rise of yield in the channels corresponding to the peak (or peaks) of the gamma ray.

Before the present experiment was performed, the region of excitation in Ne^{20} between 11 and 13 Mev was almost completely unexplored. With a variable energy deuteron beam available, up to a maximum of 2.14 Mev, the region from 11.0 to 12.5 Mev has been investigated by the technique described above, and the results are reported herein. An abstract account of a part of the present experiment has been published,⁵ and other portions of the experiment were reported orally.⁵ A resume of the results has been included in a Naval Research Laboratory progress report.⁶

II. EXPERIMENTAL PROCEDURE

Targets of CaF_2 were prepared by evaporation in vacuo onto cleaned and polished Ag disks, 1.25-in.

¹ J. W. Butler, Phys. Rev. **85**, 743(A) (1952).

² J. B. Marion, Ph.D. thesis, The Rice Institute, 1955 (unpublished).

³ J. W. Butler and H. D. Holmgren, Phys. Rev. **112**, 461 (1958).

⁴ J. W. Butler, L. W. Fagg, and H. D. Holmgren, Phys. Rev. **113**, 268 (1959).

⁵ J. W. Butler, Phys. Rev. **98**, 241(A) (1955).

⁶ J. W. Butler and H. D. Holmgren, Naval Research Laboratory Quarterly Nuclear Science and Technology, January, 1955 (unpublished), p. 2.

diam \times 0.010-in. thick. The target thicknesses used ranged from 100–500 micrograms/cm² corresponding to energy losses of about 20–100 kev for 1.5-Mev deuterons. Most of the data were taken with a 50-kev thick target. The deuterons were supplied by the NRL Nucleonics Division 2-Mv Van de Graaff accelerator. The gamma-ray spectrometer consisted of two NaI(Tl) crystals, 1.75 in. \times 1.75 in. and 3 in. \times 3 in., two DuMont multiplier phototubes, 6292 and K1197, a 20-channel differential pulse-height analyzer, and associated electronic equipment, including time coincidence circuits.

Since the gamma rays of interest were quite high in energy (9–13 Mev), a large fraction of the pulses resulting from pair creation in the crystal did not lead to "photopeak" or "total absorption" counts because of bremsstrahlung emission by members of the pair traveling through the sodium iodide, conventional wall effects, etc. In an effort to recapture some of the energy emitted in the form of bremsstrahlung, two crystals were used "in line" with the target. The two crystals were placed at 90° with respect to the deuteron beam as illustrated in Fig. 1. At high energies, the most probable direction for bremsstrahlung emission is along the direction of motion of the electron, and the most probable directions for the two members of a created pair make a relatively small angle with respect to the direction of the gamma-ray quantum. Therefore, the larger crystal was placed "behind" the smaller crystal to capture as much as possible of the bremsstrahlung radiation coming from the smaller crystal. The anodes of the two phototubes were connected together and the gains carefully balanced. A coincidence requirement was placed on pulses to be accepted for counting. A minimum of 0.8 Mev was required to be deposited in each crystal before a pulse was accepted for analysis, the individual pulses for coincidence purposes being taken from the No. 10 dynodes of the phototubes. The 20-channel analyzer, which measured the spectrum of the combined anode pulses, was gated on by the coincidence pulse, the coincidence circuit having a resolving time of 1 μ sec.

For the data taken at the lowest bombarding energies (where the gamma-ray yield was very low), the crystals were placed as close as possible to the target. But at somewhat higher bombarding energies (where the gamma-ray yield was fairly high), it was not necessary to place the crystals so close to the target. And since the corresponding neutron yield was also high, it was very desirable to use a neutron deflector between the target and the crystals. This was accomplished with the use of a truncated cone of paraffin. Above about 0.8 Mev, a Pb collimating cone was used in addition to the paraffin. The effect of the Pb cone was to shield the outer parts of the first crystal from direct illumination by the gamma rays, thus decreasing the wall effects and the escape of annihilation radiation from the crystal sides.

In addition to the Pb collimator and paraffin neutron deflector, at the higher bombarding energies an alumi-

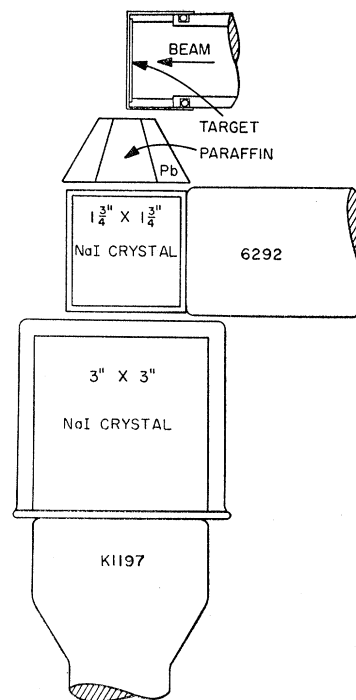


FIG. 1. Geometrical arrangement of target and NaI crystals. Signals on the No. 10 dynodes of the phototubes triggered a coincidence gate which turned on the 20-channel analyzer. The two anodes were connected together, and the combined pulse was analyzed. The paraffin served as a neutron deflector.

num attenuator (not shown) was used to decrease the intense low-energy gamma-ray yield, for example, the 1.63-Mev gamma ray, resulting from the de-excitation of the 1.63-Mev state of Ne^{20} . This state is fed by three channels: the (d, n) reaction directly, gamma-ray cascades from higher states of Ne^{20} , and the decay of F^{20} formed by the competing $\text{F}^{19}(d, p)\text{F}^{20}$ reaction. The thickness of the Al shield varied from $\frac{1}{4}$ in. up to 2 in.

The gamma-ray spectrum was displayed on the 20-channel analyzer at each bombarding energy used. The calibration factors used varied from 150 to 300 kev per channel, and the threshold of the 20-channel sweep was set in the 6–8 Mev range.

Because the yield from the reaction increased rapidly as a function of deuteron energy, and because the gain of the phototube was observed to be a function of counting rate (or phototube current) it was necessary to take precautions to insure gain stability from one bombarding energy to another. The 3.09-Mev gamma ray from the $\text{C}^{12}(d, p\gamma)\text{C}^{13}$ reaction gave an outstanding peak in the gamma-ray spectrum, and was therefore used as a check on gain stability. A liquid nitrogen cold trap was used between the target and the magnetic beam analyzer, but this did not completely prevent the formation of a thin carbon film on the target, and the relatively high cross section of the $\text{C}^{12}(d, p\gamma)\text{C}^{13}$ reaction made the intensity of the 3.09-Mev gamma ray sufficient to enable rather precise calibration measurements to be made. (A later adaptation of the cold trap target protection technique⁷ proved much more effective in preventing

⁷ J. W. Butler and C. R. Gossett, Phys. Rev. **108**, 1473 (1957).

carbon, fluorine, and other contaminants from forming on the target.)

Before and after the spectrum was obtained at each different bombarding energy, the linear amplifier gain and pulse-height analyzer threshold were changed to display the 3.09-Mev peak on the 20 channels. If the position of the peak had shifted slightly between bombarding energies, the phototube high voltage was changed slightly to bring the peak back into the same channel as before. The beam was on the target continuously, thus eliminating possible systematic changes in phototube gain with periodic changes in gamma-ray intensity.

III. RESULTS

Of the various reactions possible when F^{19} is bombarded with deuterons, the (d,n) reaction has the highest Q value (except for radiative capture of the deuteron, which has a very low cross section and has not been observed). The (d,α) reaction has almost as high a Q value, but at a bombarding energy of 1.8 Mev, the highest energy state observed to be excited in the reaction was 6.869 Mev.⁸ Because of Coulomb effects, one would not expect to observe states excited in the residual nucleus as a result of the emission of low-energy "threshold" alpha particles. The (d,p) reaction on F^{19} has a Q value of 4.377 Mev, the (d,p) reaction on C^{12} has a Q value of 2.721 Mev, and the (d,n) reaction on C^{12} has a negative Q value. (The prompt gamma rays following neutron capture in the NaI crystal were observed to exhibit a spectrum which decreases rapidly with increasing energy, having a cutoff at about 6–7 Mev.) Therefore, it is reasonable to expect that essentially all the gamma radiation above about 6–7 Mev was due to the $(d,n\gamma)$ reaction.

The thresholds are illustrated graphically in Fig. 2. Because of the very wide dynamic range of the yield over the interval of bombarding energies the detectors were used at several distances from the target, with

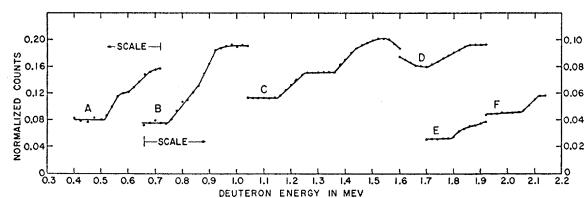


FIG. 2. The "normalized" high-energy gamma-ray counts as a function of bombarding energy. For the different regions of the curve, the following information is given: the ordinate scale (left or right) and the energy windows used to obtain the ordinate value (the numerator and denominator). A—left scale, 8.7–10.0 and 6.4–11.4 Mev. B—right scale, 9.5–11.5 and 6.3–11.5 Mev. C—right scale, 10.0–11.3 and 7.3–12.5 Mev. D—right scale, 10.5–11.8 and 7.8–13.0 Mev. E—right scale if numbers are multiplied by five, 9.8–10.8 and 7.8–13.0 Mev. F—right scale, 12.0–13.0 and 9.0–13.2 Mev. The reasons for these energy windows and the method of analysis are discussed in the text. The existence of thresholds at 0.60 and 0.85 Mev is not certain.

⁸ H. A. Watson and W. W. Buechner, Phys. Rev. **88**, 1324 (1952).

TABLE I. Summary of neutron thresholds observed in the $F^{19}(d,n\gamma)Ne^{20}$ reaction. The energies of the excited states were calculated from the known mass values and the presently measured Q values. The gamma-ray energies are the presently measured values. There is some doubt concerning the existence of the thresholds labeled with a question mark.

Deuteron energy at threshold (Mev)	Q value (Mev)	Excited state in Ne^{20} (Mev)	Energy of gamma ray (Mev)
0.51 ± 0.02	-0.46 ± 0.02	11.11 ± 0.02	9.6 ± 0.3
0.60 ± 0.02 ?	-0.54 ± 0.02 ?	11.19 ± 0.02 ?	9.7 ± 0.3 ?
0.76 ± 0.02	-0.69 ± 0.02	11.33 ± 0.02	11.5 ± 0.3
0.85 ± 0.02 ?	-0.77 ± 0.02 ?	11.42 ± 0.02 ?	11.5 ± 0.3 ?
1.15 ± 0.02	-1.04 ± 0.02	11.69 ± 0.02	11.6 ± 0.3
1.35 ± 0.02	-1.22 ± 0.02	11.87 ± 0.02	11.8 ± 0.3
1.70 ± 0.02	-1.54 ± 0.02	12.19 ± 0.02	12.0 ± 0.3
1.79 ± 0.02	-1.62 ± 0.02	12.27 ± 0.02	10.8 ± 0.3
2.06 ± 0.02	-1.86 ± 0.02	12.51 ± 0.02	12.6 ± 0.3

different amounts of absorber, different target thicknesses, etc. Furthermore, the gamma-ray energies at threshold were changing with excitation energies in the Ne^{20} excited nucleus, and hence with bombarding energies. Therefore, the "excitation curve" is not continuous over the entire range of bombarding energies.

The ordinate values of Fig. 2 represent the ratio of counts corresponding to total absorption channels for transitions to the ground state and the 1.63-Mev state to the counts in all 20 channels of the analyzer. The positions of the changes in slope are interpreted to be the threshold bombarding energies. These values are listed in Table I, together with their uncertainties, the corresponding Q values, and the excitation energies in Ne^{20} .

For curve A in Fig. 2, the plotted points correspond to the number of counts in the gamma-ray energy interval, 8.7–10.0 Mev, divided by the number of counts in the interval, 6.4–11.4 Mev. The proper ordinate scale for interval A is on the left of the graph. The first break in the curve occurs at a bombarding energy of 0.51 ± 0.02 Mev, corresponding to a neutron threshold, leaving the Ne^{20} nucleus excited by 11.11 ± 0.02 Mev. The latter value was obtained by making use of the Q value for the $F^{19}(d,n)Ne^{20}$ reaction, 10.646 Mev, which was in turn obtained from the mass values of Wapstra.⁹

The gamma-ray energy associated with this first break was measured to be 9.6 ± 0.3 Mev by taking the difference in spectra above and below the break. Specifically, the spectra at bombarding energies of 0.56, 0.58, and 0.60 Mev were added together, channel by channel, in order to obtain the spectrum well above threshold with good statistics. The spectra corresponding to bombarding energies from 0.40 to 0.50 Mev were similarly added together. The two different spectra were then normalized to the same number of total counts, and the aggregate spectrum below threshold subtracted from the one above. This difference spectrum then gives a measure of the gamma ray (or gamma rays) giving rise to

⁹ A. H. Wapstra, Physica **21**, 367 (1955).

the threshold. The measured value of the gamma-ray energy, 9.6 ± 0.3 Mev, corresponds to a transition from the excited state at 11.11 Mev to the lowest excited state in Ne^{20} , 1.63 Mev.

A probable second break occurs at a bombarding energy of 0.60 ± 0.02 Mev, corresponding to an excited state in Ne^{20} at 11.19 ± 0.02 Mev, and indicating a gamma-ray energy of 9.7 ± 0.3 Mev. This energy is also consistent with decay to the 1.63-Mev state.

Since the gamma-ray energy associated with the next threshold (0.76 ± 0.02 Mev, curve B), was considerably higher than those shown by curve A, the energy interval chosen for the plot was also different. Curve B represents the counts in the gamma-ray energy interval 9.5–11.5 Mev, normalized by dividing by the counts from 6.3 to 11.5 Mev. The proper ordinate scale for curve B is on the right side of the graph. The gamma-ray energy associated with the 0.76-Mev threshold was determined to be 11.5 ± 0.3 Mev by the same technique described above for the thresholds represented by curve A. This energy indicates a ground-state transition.

At 0.85 ± 0.02 Mev of bombarding energy, another change in slope occurs and probably represents a neutron threshold corresponding to a state in Ne^{20} at 11.42 ± 0.02 Mev. The residual excited state emits a gamma ray whose energy was measured to be 11.5 ± 0.3 Mev, a transition to the ground state.

For curve C (ordinate on right side), the plotted points represent the counts in the interval 10.0–11.3 Mev normalized by dividing by the counts in the interval 7.3–12.5 Mev. The two breaks shown, 1.15 and 1.35 Mev, represent states in Ne^{20} at 11.69 ± 0.02 and 11.87 ± 0.02 Mev, and are associated with gamma rays whose energies were measured to be 11.6 ± 0.3 and 11.8 ± 0.3 Mev, respectively. These correspond to ground-state transitions.

Curve D (ordinate on right side) shows the counts in the interval 10.5–11.8 Mev normalized by the counts in the interval 7.8–13.0 Mev. The threshold at 1.70 ± 0.02 Mev corresponds to a state in Ne^{20} at 12.19 ± 0.02 Mev emitting a gamma ray whose energy was measured to be 12.0 ± 0.3 Mev, a ground-state transition.

For curve E, the numbers on the right-hand ordinate scale should be multiplied by five. The normalized counts are higher than for the other curves because the gamma-ray transition is to the 1.63-Mev state of Ne^{20} , and the energy window including the usual three peaks from such a transition also includes a considerable number of counts corresponding to higher energy gamma rays. The intervals used were 9.8–10.8 and 7.8–13.0 Mev. The threshold bombarding energy was measured to be 1.79 ± 0.02 Mev, and the gamma-ray energy measurement was 10.8 ± 0.3 Mev, indicating decay to the 1.63-Mev state of Ne^{20} .

The highest energy threshold observed is at 2.06 ± 0.02 Mev, residual excited state energy, 12.51 ± 0.02 Mev, and is shown by curve F (right hand ordinate). The energy windows used were 12.0–13.0 and 9.0–13.2 Mev,

and the gamma-ray energy was measured to be 12.6 ± 0.3 Mev, thus indicating a ground-state transition.

The excited states corresponding to neutron thresholds found in the present experiment are shown schematically in Fig. 3. Also shown are the observed modes of decay.

IV. DISCUSSION

Since the binding energy of the last alpha particle in Ne^{20} is 4.753 Mev,⁹ any excited state above this value can decay by either alpha emission or gamma-ray emission, as far as energy requirements are concerned. Since O^{16} and the alpha particle both have zero spin, an excited state in Ne^{20} having a high spin value might be expected to have a relatively narrow alpha-particle partial width because of the centrifugal and Coulomb barriers. An odd-parity state in Ne^{20} with even spin, or an even-parity state with odd spin could not decay into an alpha particle and O^{16} in the ground state because of the spin-parity conservation requirements. And finally a $T=1$ state in Ne^{20} could not decay by alpha emission leading to a $T=0$ state in O^{16} (in particular, the ground state) if the simple application of isobaric spin selection rules are quantitatively valid in this case.

Thus, even though the excited states of interest to the present discussion are unstable for alpha emission by about 7 Mev (and without the considerations discussed in the above paragraph, would be expected to decay almost exclusively by alpha emission), it is reasonable to expect to find states in the region which have appreciable probability for decay by gamma emission. Indeed, this is the basis on which the present experiment was performed.

Another conceivable method of detecting states in the region of excitation in the present experiment is by observing alpha-particle groups from the $\text{F}^{19}(d, n\alpha)\text{O}^{16}$ experiment. This reaction, however, has the inherent

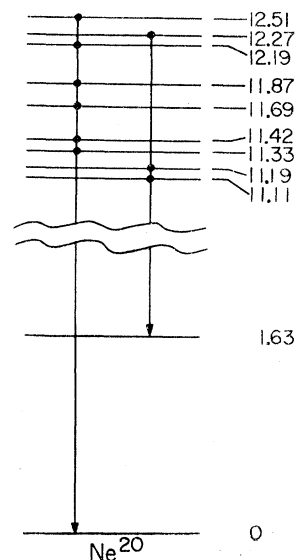


FIG. 3. The excited states in Ne^{20} found in the present experiment and their observed modes of decay.

disadvantage of "smearing out" the particle groups because some of the disintegrations would involve three-body breakup. It is conceivable, however, that the partial width for neutron emission might be sufficiently greater than that for alpha-particle emission that the majority of such three-body breakups would proceed by two steps sufficiently separated in time that the neutron leaves the residual Ne^{20} nucleus in a well-defined state, which subsequently decays by alpha emission. The alpha-particle energies would still be influenced, however, by the angle between neutron and alpha emission. Thus some smearing of alpha-particle groups is inevitable.

Watson and Buechner⁸ analyzed the alpha-particle groups from the $\text{F}^{19}(d,\alpha)\text{O}^{17}$ reaction. Since the above-mentioned $\text{F}^{19}(d,n\alpha)\text{O}^{16}$ reaction completes with the reaction observed by Watson and Buechner, the alpha-particle groups from the latter reaction would be present in their alpha-particle spectrum. They did observe a broad distribution of alpha particles and assumed this distribution to arise from the $\text{F}^{19}(d,n\alpha)\text{O}^{16}$ reaction. Under this assumption, they calculated the value of the highest state in Ne^{20} leading to this distribution to be 11.85 Mev. This value is in good agreement with the excited state corresponding to the 1.35-Mev threshold of the present experiment, 11.87 Mev. The agreement is improved if one corrects their value by recalculating it, using the presently accepted value⁹ of the mass difference between Ne^{20} and O^{16} plus an alpha particle, 4.753 Mev. The Ne^{20} excited state of Watson and Buechner then becomes 11.87 Mev.

We examined their published curve for possible alpha-particle groups corresponding to other states observed in the present experiment. We did find two possible weak alpha-particle groups in the continuum, and after converting the $H\rho$ values obtained from their curve to energy excitation values, we obtained 11.44 and 11.34 Mev for excited states in Ne^{20} . If these values are significant, they correspond to the thresholds at 0.85 and 0.76 Mev in the present experiment, the excited states being 11.42 ± 0.02 and 11.33 ± 0.02 Mev. The two highest states in Table I could not have corresponding alpha-particle groups in the curve of Watson and Buechner because their bombarding energy was 1.8 Mev, just at the threshold corresponding to the 12.27-Mev state. One would therefore not expect to find much yield of this state at that energy, and of course would expect no yield of any higher energy states. If there were alpha-particle groups corresponding to the two lowest states of Table I, they were obscured by an intense alpha-particle group from the $\text{F}^{19}(d,\alpha)\text{O}^{17}$ reaction.

According to the selection rules, excited states in Ne^{20} , having $T=1$, can be produced by the $\text{F}^{19}(d,n)\text{Ne}^{20}$ reaction, and for reasons discussed above, one would expect that some states having an appreciable probability for decay by gamma radiation (in the energy region of interest) would be $T=1$ states. (The lowest energy $T=1$ state in Ne^{20} is believed to be the 9.97-Mev state.¹⁰)

If one compares the known-level density in F^{20} below about 2.5 Mev (all $T=1$ states) with the known-level density in Ne^{20} from about 10 to about 12.5 Mev (the corresponding region if the 9.97-Mev state in Ne^{20} is the first $T=1$ state), one finds that there are eight such states in F^{20} , and there are nine states in the corresponding region of Ne^{20} from the results of the present experiment. In addition, there is a possible $T=1$ state in Ne^{20} at 10.61 Mev.¹⁰ Thus, probably most, if not all, of the states found in the present experiment are $T=1$ states. As mentioned above, the application of the simple isobaric spin selection rules forbids such $T=1$ states from emitting alpha particles to the ground state of O^{16} . However, in practice, one usually finds some configuration mixing and some degree of isobaric spin impurity. Therefore, the naive application of the rules is seldom quantitatively valid. So the possible weak alpha-particle groups mentioned above from the work of Watson and Buechner do not necessarily mean that they cannot correspond to $T=1$ states. Although there probably do exist states in this region which are predominantly alpha emitters, they would not necessarily appear prominent in the alpha-particle spectrum from the deuteron bombardment of F^{19} because the population of such states would first be dependent on the proton width of the state in Ne^{20} (assuming the direct process mechanism) or the neutron width of the compound state in Ne^{21} (assuming the compound nucleus model).

The alpha-particle scattering by O^{16} has been measured up to a bombarding energy of about 5.5 Mev,^{11,12} corresponding to an excitation in Ne^{20} of about 9 Mev. Therefore, no direct comparison can be made between states observed in the $\text{O}^{16}(\alpha,\alpha)$ reaction and those of the present experiment.

Terrell and Phillips¹³ measured the gamma-ray spectrum from the $\text{F}^{19}(d,n\gamma)\text{Ne}^{20}$ reaction at a bombarding energy of 1.56 Mev, and reported a gamma ray of 11.5 ± 0.4 Mev. Bent et al.,¹⁰ using the same reaction but at a bombarding energy of 3.6 Mev, reported gamma rays of 11.51 ± 0.2 and 10.61 ± 0.1 Mev. These gamma-ray energies can be fitted into the level scheme observed in the present experiment, but the uncertainties in the gamma-ray energies are approximately equal to the level spacing, so a unique assignment cannot be made.

Marion,² using the $\text{F}^{19}(d,n)\text{Ne}^{20}$ reaction, the neutron ratio technique,² and a CaF_2 target, found evidence for several neutron thresholds between bombarding energies of 1 and 5 Mev. But it was not definitely established that these thresholds were due to F^{19} . Only one of these thresholds was below 2 Mev, its energy being 1.487 ± 0.010 Mev. Since it does not correspond to any of the

¹⁰ R. D. Bent, T. W. Bonner, J. H. McCrary, W. A. Ranken, and R. F. Sippel, *Phys. Rev.* **99**, 710 (1955).

¹¹ J. R. Cameron, *Phys. Rev.* **90**, 839 (1953).

¹² L. C. McDermott, K. W. Jones, H. Smotrich, and R. E. Benenson, *Bull. Am. Phys. Soc.* **3**, 199 (1958).

¹³ N. J. Terrell and G. C. Phillips, *Phys. Rev.* **83**, 703 (1951).

thresholds found in the present experiment, either (1) it was not due to F^{19} or (2) the residual state does not decay by gamma emission principally to the ground state or first excited state of Ne^{20} .

ACKNOWLEDGMENT

The author wishes to express his sincere appreciation to Dr. H. D. Holmgren for his help in the making of the experimental measurements.

Radioactive Decay of Lu^{168}

R. G. WILSON AND M. L. POOL

Department of Physics and Astronomy, Ohio State University, Columbus, Ohio

(Received October 26, 1959)

Ytterbium oxide enriched to 30.9% in the 168 mass number was irradiated with 6-Mev protons. An activity decaying by electron capture with a half-life of 7.1 ± 0.2 minutes was produced and assigned to Lu^{168} . The activity consists of gamma rays with energies of 87 ± 1 , 900 ± 7 , 987 ± 7 , 1410 ± 20 , 1800 ± 40 , 2130 ± 60 kev in addition to the ytterbium K x ray. An energy level scheme for this decay is presented.

YTTERBIUM oxide enriched to 30.9% in the 168 mass number was irradiated with 6-Mev protons. The initially resulting activity is assigned to Lu^{168} by the identification of the ytterbium K x ray and by comparison with the activities produced by similar proton irradiations of each of the other enriched isotopes of ytterbium. Each of these irradiations produced the well known lutetium activity with the same mass number as the irradiated ytterbium isotope by a (p, n) reaction with no evidence of other reactions. The initial activity observed following the irradiation of Yb^{168} was different from all of the activities produced by the irradiations of the other enriched isotopes of ytterbium. It is assumed that this activity was also produced by a (p, n) reaction.

The observed activity of Lu^{168} consists of the ytterbium K x ray and gamma rays with energies of 87 ± 1 , 900 ± 7 , 987 ± 7 , 1410 ± 20 , 1800 ± 60 , and 2130 ± 80 kev. From an analysis of the decay of the annihilation radiation in the gamma-ray spectrum of this activity, it is concluded that if positron radiation exists in the activity of Lu^{168} , it results from less than 1% of the disintegrations of Lu^{168} and that the mode of decay of Lu^{168} is therefore essentially by electron capture to Yb^{168} . The half-life of Lu^{168} is 7.1 ± 0.2 minutes as measured by following the decay of the individual gamma rays for over six half-lives with a scintillation spectrometer. The approximate ratios of the relative numbers of the observed radiations in the activity of Lu^{168} after correction for crystal counting efficiency are K x ray:87-kev γ :900-kev γ :987-kev γ = 100:7.5:10:13. The remaining three gamma rays are weak.

The energies of the established first rotational levels of even-even nuclei in the region of Yb^{168} are between 76 and 95 kev; in particular, those of the other even-even nuclei of ytterbium are 84, 79, 77, and 82 kev in order of increasing mass number. It therefore seems probable that the 87-kev transition observed in the

activity of Lu^{168} proceeds from the first rotational level to the ground state of Yb^{168} . Thus an 87-kev $2+$ level is tentatively assigned to Yb^{168} . Because the energy difference between the 900- and 987-kev gamma rays is the same as that of the now assigned first rotational level of Yb^{168} , a 987-kev level of spin 1 or 2 is tentatively assigned to Yb^{168} .

${}_{71}\text{Lu}_{97}^{168}$ is in the region of elliptically deformed odd-odd nuclei. Shell theory predicts spins of $1-$ and $6-$ for this nucleus using the measured spins of ${}_{71}\text{Lu}^{175}$ and ${}_{66}\text{Dy}_{97}^{168}$ which are $7/2+$ and $5/2-$, respectively. Because gamma rays corresponding to transitions between rotational levels in Yb^{168} above the first are not observed in the activity of Lu^{168} , the choice of $1-$ is favored for the ground state of Lu^{168} .

Assuming the 87-kev transition to be E_2 , its K , L_1 , L_2 , L_3 , and M internal conversion coefficients are 1.20, 0.13,

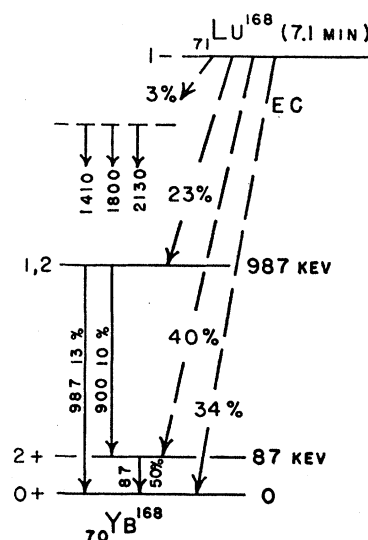


FIG. 1. Proposed energy level scheme for the decay of Lu^{168} .